A Hybrid Method for Fetal Heart Rate Classification

Akhil Masurkar
Department of Electronics and Computer Science
Vidyalankar Institute of Technology
Mumbai, India

Gaurav Gaonkar
Department of Computer Engineering
Vidyalankar Institute of Technology
Mumbai, Maharashtra, India

***Abstract*— Fetal heart rate (FHR) is an essential parameter for long-term prenatal monitoring of intrauterine fetal health. FHR, if measured correctly, can help reduce incidences of miscarriage and infant mortality and detect potential heart problems before delivery. The present study aims to create an automatic fetal heart rate diagnosis system. A novel technique is used to predict the fetus's health using raw audio signals acquired from an electronic stethoscope. Adaptive bandpass filtering based on extracted Continuous Wavelet Transform (CWT) coefficients is used to filter the input signals. The filtered signal is used to extract features such as pitch frequency, beats per minute (BPM), recurrent quantification analysis (RQA) features, and chroma vector to generate a suitable data set that trains a Gradient Boosting Classifier. Our proposed system shows improved results from existing FHR classification techniques and performs with an accuracy of 94.3%. This technique shall assist the doctor and health care workers in monitoring fetal health regularly and taking timely action in case of an aberration.**

***Index Terms*— Fetal Heart Rate, Shannon entropy, Gradient Boosting, Recurrence Quantification Analysis, Phonocardiogram signals, Adaptive Bandpass Filtering**

I. INTRODUCTION

Fetal heart rate assessment is the key to understand the fetus's health during or before labor. It is reported that around 3 million fetal deaths occur worldwide every year. The precise diagnosis of at-risk pregnancies can significantly prevent fetal deaths. Fetal Monitoring systems help to reduce the mortality rate substantially this system are commonly known as Electronic Fetal Monitoring EFM. EFM was first introduced at Yale University USA in 1958 [2]. Since then, EFM has been the most shared obstetric practice during labor.

The EFM involves Cardiotocography (CTG), which monitors and measures the fetal heart rate and mother's contractions during labor with an ultrasound machine and a pressure sensor. CTG consists of the intrauterine pressure (IUP) and fetal electrocardiogram (FECG) signals to measure uterine contraction and FHR. The signals sent from these sensors are displayed on the computer screen, often known as EFM tracings, and the changes in uterine contractions on standard fetal heart rate are observed precisely. The autocorrelation method [3] is the most used approach for the FHR analysis in CTG monitoring. EFM generates various graphs which helps predominantly in graphical analysis of FHR patterns [4]. Due to the introduction of CTG monitoring, the extent of birth asphyxia has been reduced immensely. On the contrary, it has also contributed to the drift of the cesarean section [5]. The rise in the cesarean section has resulted from a poor understanding of CTG signals' correspondence with fetal behavior. New policies by the NICHD (National Institute of Child Health and Human Development) were introduced for CTG monitoring to enhance the interpretations of CTG signals and decline the rate of acidosis and cesarean sections [6]. Regardless of the policies[7], the poor rendition of CTG persists.

Among all the monitoring techniques, Fetal Phonocardiography (FPCG) possesses the least harm to the antepartum (before childbirth) and intrapartum (during labor) care. A fetal phonocardiogram records the fetal heart sounds (FHS) produced by different cardiac chambers for pulsating and moving blood throughout the cardiac cycle [8]. Previous FPCG based FHR classification methods are primarily dependent on the calculation of time difference between detected successive heart beats. However, their performance stands low due to inadequate sound quality in low signal and noisy areas [9].

We propose a novel technique for the FHR classification from FPCG. Firstly, our proposed system aims at removing noise and sporadic interferences that mix with the signal audio during recording. The resultant signal is cleaned and denoised enough to extract the fetal heartbeat signal. The fetal heartbeat is extracted using peak detection and beat localization by adding a de-bounding condition. The frequency contents, spectral features of the cleaned fetal heart signal, and corresponding beats per minute (numeric value) of various subjects serve as a data set. The data set is pre-processed and used to train a classifier for predicting the fetal health. Section II gives the overview of the related work done in this area of FHR monitoring. Section III describes the database used in this research. Section IV elaborates on our proposed system with flow diagram and detail explanation. The filtering and feature extraction processes are discussed in section V. Section VI explains feature selection, hyperparameter tuning process and compares the performance of different machine learning classifiers. Sections VII highlights the performance of the selected classifier on the relevant classification metrics. In section VIII we conclude and discuss the possible advancements in this research.

II. LITERATURE REVIEW

The significant step in FHR classification is identifying notable features from the FHR-IUP signals that can accurately detect the unique FHR patterns. In [10], V. Chuda Cek provides a thorough study of such important features for FHR analysis. These features consist of morphological features [11], linear features such as mean and variance, and nonlinear features, for example, fractal dimension (FD) [12], power spectral density estimates [13]. In [14], P. A. Warrick et al. focus on the dynamic relationship between the IUP and FHR signals. Using a system identification method to evaluate the dynamic relationship as an impulse response function. For FPCG filtering, wavelet-based approaches have been proposed due to their adaptable and efficient nature. Chourasia and Tiwari [15] designed a new adaptable and robust wavelet basis function for Discrete Wavelet Transform based FPCG denoising. In their studies, the newly developed Mother Wavelet provided better results in FPCG denoising. Koutsiana et al. [16] used a Fractal Dimension (FD) analysis in the wavelet domain to remove background noise from various simulated fetal heart recordings. While this approach shows promising results, it remains untested on actual recordings. In [17], Kovacs et al. suggested an acoustic method for real-time and long-term fetal heart monitoring using a portable electronic device that underwent testing in clinical practice. However, due to the limitations of the acoustic approach, it becomes impossible to extract FHR information from certain sections of the recording. A comprehensive approach for FHR classification mentioned in [18], Dash et al. uses generative models and Bayesian theory for FHR classification. The rule-based machine learning classifiers for FHR classification have been discussed in [9] and neural networks [19]. In [20], V. Chuda Cek proposed a machine learning approach for FHR classification approach using PCA (principal component analysis) followed by a direct correlation of important feature sets with fetal heart rate. The feature-based FHR classification using machine learning is mentioned in Akhil Masurkar et al. [21], uses a Shannon energy envelope-based beat localization algorithm and other prime factors in pregnancy for FHR classification.

III. DATA SET

The fetal heart sound database acquired by Shiraz University (SU) [22] is used in this research. The database includes fetal heart sound recordings from 109 pregnant women recorded with an electronic stethoscope. It consists of 119 recordings with a 16,000 Hz sampling rate and a few at 44,100 Hz and 16-bit quantization. The data set is unevenly distributed within two classes with distribution split of 75% for Normal and 25% for Abnormal class. Originally the average duration of each sample was around 90 seconds. We clipped the audio files into 10 seconds, generating 7 to 9 new samples from each previous recording. Generate a total of 862 samples of 10 seconds each after clipping the audio files from the original database.

IV. PROPOSED SYSTEM

The proposed system is based upon phonocardiography for fetal health monitoring. Once the phonocardiogram signal serves as the input to the system, it is subjected to filtering, i.e., It is denoised using continuous wavelet transform (CWT) and an adaptive bandpass filtering (BPF). Once the fetal heart audio signal is filtered, our system generates 20 features using pre-processing techniques. The signal goes through feature extraction processes such as Beats per Minute localization, Recurrent Quantification Analysis, chroma features, and frequency contents. Once features are established, they are used for classification, using Gradient Boosting Classifier (GBC) to predict on any new data based on existing data trends and tendencies. Fig 1. Show the flowchart of our proposed system.

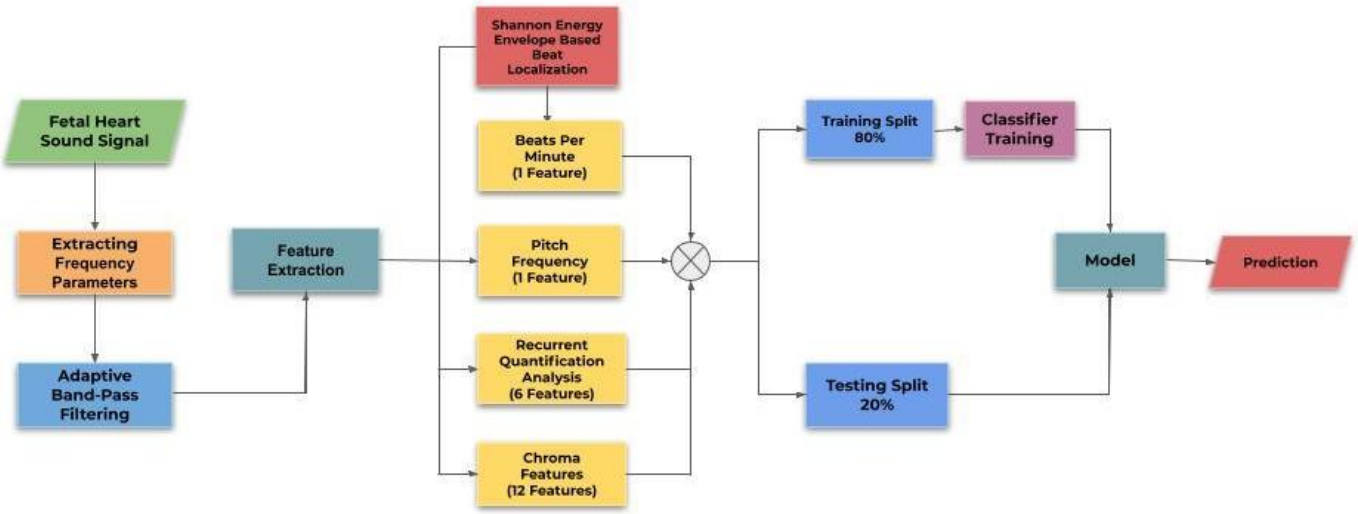

Fig 1. Shows the flow chart of our proposed system

V. METHODOLOGY

This section describes the specific procedures involved in the proposed FHR classification technique. It illustrates the basic principles of the techniques used for the feature extraction process, such as Signal filtering, Shannon energy envelope-based beat localization, RQA, Chroma vector, and Beat Per Minutes. The flow diagram of the proposal is shown in Fig 1.

A. Signal Analysis

Continuous wavelet transform (CWT) is used to design the filtering algorithm. The Analytical Morlet (Gabor) wavelet is selected due to its morphological resemblance to a fetal heartbeat. A discretized version of CWT is used to increase computational speed. The magnitude scalogram below shows that the scales corresponding to 250-500 Hertz have the most signal energy, correlating to the heartbeats. Any other frequency scale corresponds to the unwanted sporadic occurrences in the signal magnitude (noise).

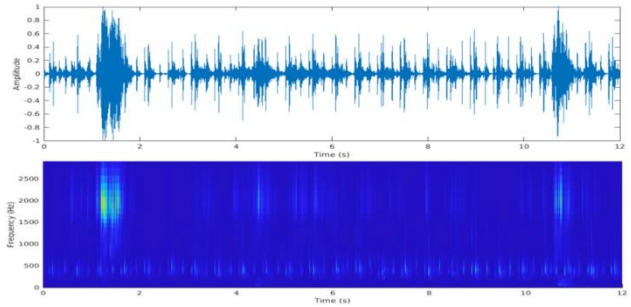

Fig 2. Shows comparison of sample f72_1 and its CWT Magnitude Scalogram

The frequency range for the desired audio of each signal is calculated using CWT coefficients. The scale magnitude of every sample in time is extracted. Next, a smooth curve is obtained by point-wise summation of scale parameters for every discrete signal sample and then interpolating the values.

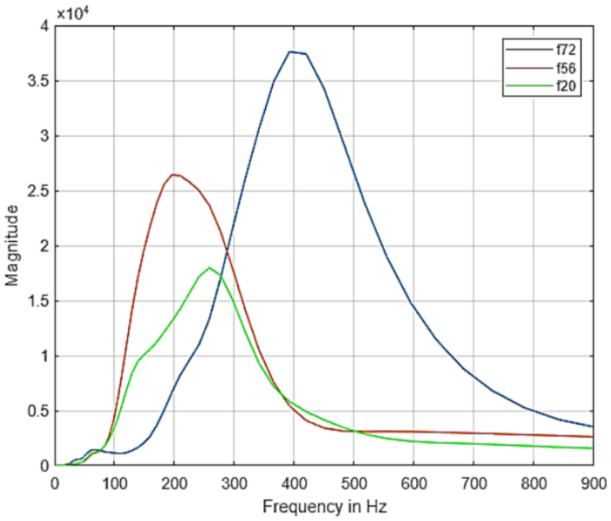

Fig 3. Shows the comparison of the sum of Magnitudes of CWT Coefficients for Samples f72_1, f56_1, f20_1

From figure 3, it is evidential that the spread of the curve for each signal is different. The peak magnitude and the frequency at which the peak occurs also vary for each signal. Having fixed filter parameters to clean every data sample may lead to a compromised signal-to-noise ratio (SNR), resulting in improper segmentation and classification.

B. Extracting Filter Parameters

The curves obtained using CWT coefficient are normalized to compensate for the varying nature of each recording, then a threshold is selected at 30% of the peak magnitude. The point when magnitude equals the threshold gives the upper and lower cut-off frequencies for the filter, shown in fig. 4 below. A Finite Impulse Response (FIR) filter is selected for its linear phase response in the pass band and constant group delay. An attenuation of 1 decibel is set for the pass band and 120 decibels for both the stop bands.

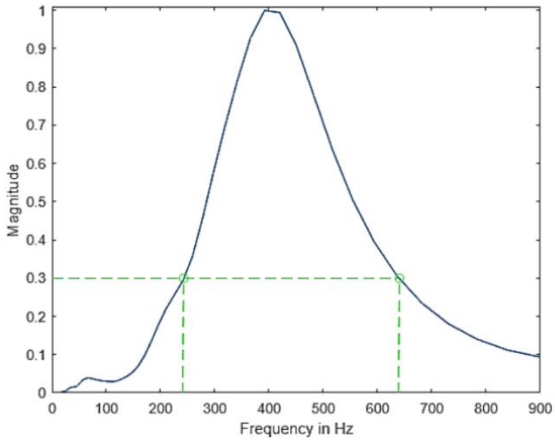

Fig 4. Shows the selection of Cut-off Frequencies for sample f72_1 after normalization and thresholding

C. Shannon Energy Envelope-Based Beat Localization

The attribute beats per minute (BPM) is extracted using Shannon Energy Envelope (SEE) based beat localization. This algorithm involves detecting the upper peaks of the filtered FHR signal. Shannon energy (SE) calculates the energy of the local spectrum for each sample present in the signal. It is evaluated by using equation (1)

$$SE = -X^2[n] * log\ log(X^2[n]) \quad (1)$$

Comparing different enveloping methods [23], Fig. 5 shows that using classic energy will attenuate sounds having lower magnitude much more than it attenuates the higher magnitude sounds (comparatively negligible). This increases the ratio of high-to-low intensities in the signal. Shannon entropy amplifies the intensities of lower amplitude sounds, thus increasing the effect of low amplitude noise, making the signal envelope too noisy to read.

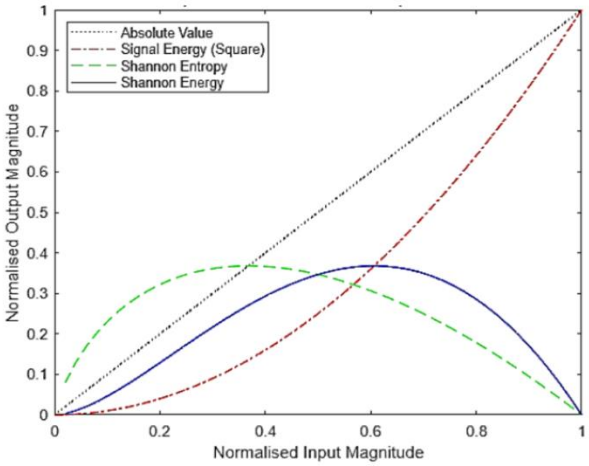

Fig 5. Shows the comparison of Different Envelope Methods

Signal energy is approximately equal to the square of the signal data $x(n)$. Hence, the signal energy of a discrete-time signal will be as given in equation (2)

$$E_x = \sum_{-\infty}^{\infty} |x(n)|^2 \quad (2)$$

Shannon energy calculates the mean spectrum of the signal, creating a frequency-dependent regulation that directly relates to the Fourier spectrum [24]. It contributes to the suppression of higher and lower intensities of the signal, and the magnitudes between the higher and lower amplitudes are made consistent. Hence, any abrupt, loud, or dull noises are suppressed, keeping the amplitudes in the middle region, where most of the vital signal lies, less attenuated. This helps in better detection of the desired signal peaks. The algorithm calculates the Shannon energy (SE) of the entire signal, and then the Shannon energy envelope is determined through spline interpolation over local maxima. The beats are localized using a predefined threshold over the Shannon energy (SE) envelope. A debounce condition is deployed to further minimize the errors caused by false peaks in the beat localization process. Results of the beat localization process are displayed in figure 6 below. Once the beats have been localized, the final beats per minute value can be calculated using the equation (3)

$$BPM = \frac{Total\ Beats * Sample\ rate\ of\ signal * 60}{Total\ no\ of\ samples\ in\ signal} \quad (3)$$

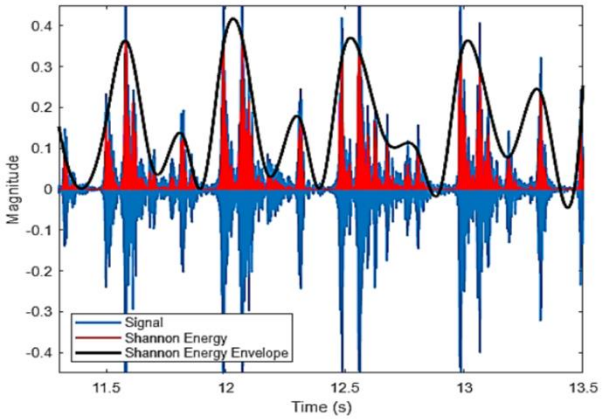

Fig 6. Shows the Original Signal and its Shannon Energy Envelope

D. Recurrent Quantification Analysis

RQA is a technique of nonlinear analysis of the dynamical system. It is based on the phase space concept, and it quantifies the differently appearing recurrence plots [25]. Recurrence Plots (RPs) is a graphical tool used to visualize a dynamic system according to its phase space trajectory. For the construction of RPs, a new phase space T is created from the original data [t1, t2, . . ., tn] of length n using time-delay and the Takens embedding theorem [26]. *T* can be reconstructed, as shown in equation (4)

$$\begin{aligned} &\{T(1) = \{t_1, t_{1+\tau}, \ldots\ldots, t_{1+(m-1)\tau}\}, \\ &\quad \ldots \\ &T(i) = \{t_i, t_{i+\tau}, \ldots\ldots, t_{i+(m-1)\tau}\}, \\ &\quad \ldots \\ &T(n-(m-1)\tau) = \{t_{n-(m-1)\tau}, t_{n-(m-2)\tau}, \ldots\ldots, t_n\} \end{aligned} \quad (4)$$

Where *T* is a square matrix of dimension m x m, and *T*(i) presents the ith row of *T* matrix, m and τ denote the embedding dimension and time delay, respectively. The recurrence matrix or the recurrent plots can be calculated using equation (5)

$$\begin{aligned} R_{i,j} &= \Theta(\varepsilon - T(i) - T(j)) \\ &= \{1 : > T(i) - T(j), \quad i,j \in [1, n-(m-1)\tau] \\ &\quad \{0 : \varepsilon < T(i) - T(j), \end{aligned} \quad (5)$$

Where $\| \cdot \|$ represents the euclidean distance (L2 norm), ε is the recurrence threshold parameter, and $R_{i,j}$ is a $n-(m-1)\tau \times n-(m-1)\tau$ matrix, and Θ (·) denotes the

Heaviside function. If the euclidean distance between T_i and T_j is less than ε, $R_{i,j}$ = 0, it creates a black pixel at position *(i,j)* in the recurrence matrix; otherwise, $R_{i,j}$ = 1. The recurrence plot of a filtered FHR sound signal is shown in Fig. 7 below

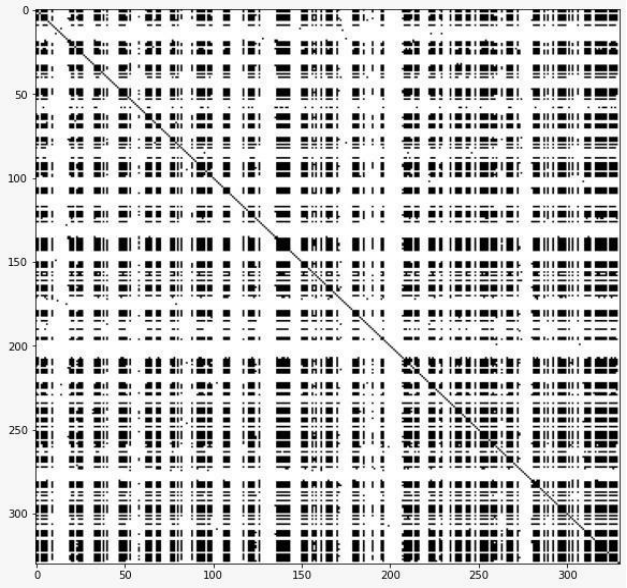

Fig 7. Shows the Recurrence Plot of fetal heart sound signal

The embedding dimension m, threshold, and time delay tau are the three essential parameters in RQA and must be tuned to construct a good recurrence plot. We used an embedding dimension of 330 in this study since it gave a good representation of the recurrence behavior present in the signal. The time delay τ is set to 2 based on the mutual information [27], and ε is empirically set to 0.8. It's highly impractical to visually understand the patterns and structures revealed by the recurrence plot. Hence, RQA is used to quantify the number and duration of small patterns within the recurrence potentials by using several recurrence statistics. In this paper, 6 features R1−R6 are derived from the RPs.

A. Recurrence Rate

Recurrence Rate (RR) is one of the most important measures of RQA. Its value represents the density of the recurrence plot. It corresponds with the probability of reoccurrence of a specific state in recurrence plot. It is expressed as shown in equation 6

$$RR = \frac{1}{N^2}\sum_{i,j=1}^{N} R(i,j) \tag{6}$$

where $R(i,j)$ is an element of the recurrence plot and N is equal to the dimension m of recurrence plot.

B. Determinism

Determinism (DET) differentiates between the organized RPs points and the dispersed ones. It measures the predictability of the dynamic system. A high value of DET indicates a steady system, while a low value denotes a stochastic system.

$$DET = \frac{\sum_{l=l_{min}}^{N} lP(l)}{\sum_{l=1}^{N} lP(l)} \tag{7}$$

Where l_{min} is the minimum length of the diagonal lines and $P(l)$ denotes frequency distribution of diagonal line.

C. Laminarity

Laminarity (LAM) is measures the chaotic transitions and it signifies the number of laminar phases in a dynamic system. It is given by.

$$LAM = \frac{\sum_{v=v_{min}}^{N} vP(v)}{\sum_{v=1}^{N} vP(v)} \tag{8}$$

where $P(v)$ is the frequency distribution of the vertical lines with a minimum length of v_{min}. LAM increases when RP consist of more recurrence point in vertical structures

D. Trapping Time

Trapping Time (TT) is the average time for which a state of RPs is recurring (trapped). TT calculates the average length of the vertical lines having minimum vertical length v_{min}, and it is given by.

$$TT = \frac{\sum_{v=v_{min}}^{N} vP(v)}{\sum_{v=v_{min}}^{N} vP(v)} \tag{9}$$

E. Shannon Entropy

Shannon Entropy (LENTR) represents the complexity of a system and it helps to estimate the required amount of information to recover the recurrence plot.

$$LENTR = -\sum_{l=l_{min}}^{N} p(l)\, ln\, p(l) \tag{10}$$

The probability $p(l)$ that a diagonal line has length l can be calculated from the frequency distribution $P(l)$

$$p(l) = \frac{P(l)}{\sum_{l=l_{min}}^{N} P(l)} \tag{11}$$

where l_{min} is the minimum length of the diagonal line and $P(l)$ is frequency distribution of the diagonal length.

F. Divergence

It measures the divergence between the phase space trajectories of a dynamical system. It calculates the amount of time for which the phase space trajectory of a dynamic system runs parallel. It is stated as the reciprocal of the maximal length of the diagonal lines. Its value corresponds to the positive

maximal Lyapunov exponent. In a dynamic system, the Lyapunov exponent represents the divergence rate of extremely close trajectories.

$$DIV = \frac{1}{L_{max}} \tag{12}$$

L_{max} denotes the maximum length of the diagonal line.

G. Chroma Vector

Chroma-based features are efficacious for interpreting music whose pitch can be categorized (often in twelve categories) and whose tuning corresponds to the equal-tempered scale. One salient property of chroma vector is it captures the harmonic and melodic features of melody while being vigorous to changes in tone and instrumentation. It represents how humans relate colors to notes. In other words, the same notes from two distinct octaves to be of the same color. Thus, we have 12 notes at windows A, A#, B, C, C#, D, D#, E, F, F#, G, and G#. These notes are not mutually exclusive; one can have more than one note for a given time frame. The chroma vector of a sample fetal heart audio using a chormogram is shown in Fig 8.

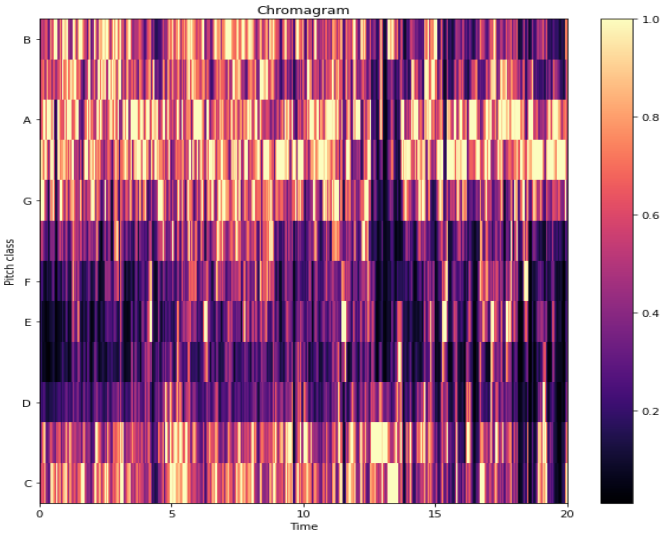

Fig 8. Show the chromagram of fetal heart sound signal

We further find the note frequency from the chroma vector. In other words, we further found out which note is being hit how many times in the signal. Fig 9. below shows the frequency plot of chroma vector.

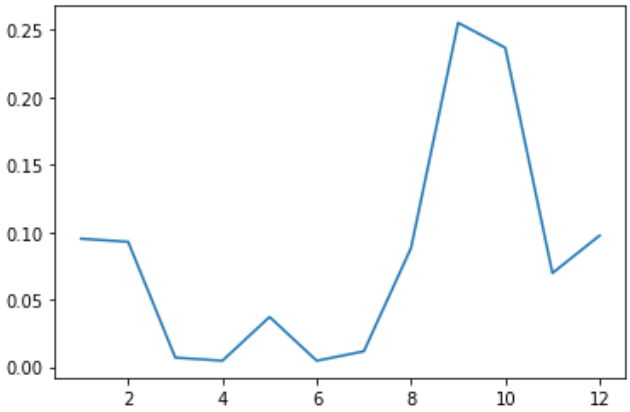

Fig 9. Shows the note frequency plot of all 12 notes

Using these extracted features, a final data set consisting of 20 features is created, which includes.

1. 12 chroma based features (frequency of 12 notes)
2. 6 RQA features (Recurrence Rate, Determinism, Laminarity, Trapping time, Shannon Entropy and Divergence)
3. Beats per minute (BPM)
4. Pitch Frequency

VI. Feature Selection and Model Hyperparameter Tuning

The pre-processed data set consists of 862 samples with a class imbalance of 75% normal and 25% abnormal categories. The 25% random samples from the normal class are selected to form a new data set to balance the uneven distribution. The new data set consists of 448 samples with equal distribution of two classes, and it is split into two sets: train and test with 80% and 20% split, respectively. A five-fold cross-validation method is used during training to obtain precise diagnostic accuracy. importance each feature is calculated using the feature importance function of the Random Forest Classifier. Feature important plot is shown in Fig 10. below.

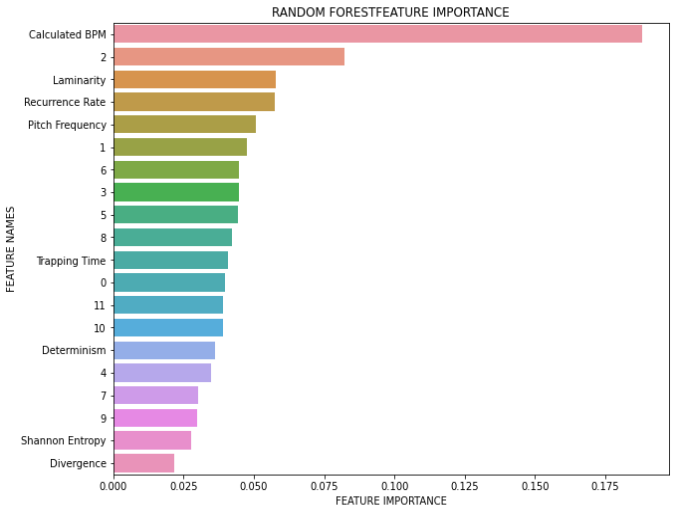

Fig 10. Shows the Feature importance plot

Top 5 most important features such as *(calculated bpm, laminarity, pitch frequency, recurrence rate and 3 notes from chroma features*) are selected as input features. Different machine learning models are trained on the selected features. Baseline accuracy of each model is compared, and the most accurate model is selected based on cross validation accuracy and further fine-tuned using Grid Search CV. The initial cross validation accuracy of the Gradient boosting classifier was 86% better than most of the models and hence it was picked for fine tuning. Initial Cross validation accuracy of machine learning models are mentioned in Table 1

Name	Test Accuracy Mean	Mean Precision	Mean Recall	Mean F1-score
GradientBoosting Classifier	**0.869**	**0.843**	**0.905**	**0.873**
XGB Classifier	0.863	0.864	0.860	0.861
Decision Tree Classifier	0.852	0.849	0.854	0.851
Bagging Classifier	0.843	0.842	0.849	0.843
AdaBoost Classifier	0.830	0.807	0.866	0.835
RandomForest Classifier	0.810	0.806	0.815	0.811
ExtraTree Classifier	0.807	0.806	0.815	0.805
KNeighborsClassifier	0.774	0.769	0.782	0.774
LinearSVC	0.751	0.736	0.781	0.757
SVC	0.749	0.732	0.781	0.755
Linear Discriminant Analysis	0.746	0.731	0.776	0.752

Table 1 shows the accuracy of top-10 machine learning models

After using the model with fine-tuned hyperparameters, the cross-validation accuracy of the Gradient Boosting Classifier went up to 93.3% performance of different models is shown in Table 2 below.

Name	Test Accuracy Mean	Mean Precision	Mean Recall	Mean F1-score
GradientBoosting Classifier	**0.93**	**0.90**	**0.97**	**0.94**
XGB Classifier	0.91	0.88	0.95	0.91
ExtraTree Classifier	0.90	0.87	0.93	0.90
Bagging Classifier	0.87	0.85	0.90	0.87
RandomForest Classifier	0.86	0.84	0.90	0.87
DecisionTree Classifier	0.84	0.83	0.866	0.849
Adaboost Classifier	0.838	0.813	0.877	0.844
NuSVC	0.768	0.730	0.855	0.785
GaussianProcess Classifier	0.765	0.750	0.800	0.772
SVC	0.757	0.736	0.805	0.768
KNN classifier	0.757	0.743	0.794	0.767

Table 2 Shows the accuracy of fine-tuned classifiers

Different feature combination such as (BPM + Pitch Frequency + RQA), (BPM + Chroma + Pitch Frequency), (Chroma + RQA) and (BPM + Pitch Frequency + Chroma + RQA) were considered and different machine learning model were trained on each feature combination. Table 3 shows the top accuracy on each feature combination.

Name	Top-Test Accuracy	Precision	Recall	F1-score
BPM + Chroma + Pitch Frequency)	0.877	0.850	0.910	0.881
(BPM + Pitch Frequency + RQA)	0.888	0.870	0.910	0.891
(Chroma +RQA)	0.800	0.846	0.733	0.812
(BPM + Pitch Frequency + Chroma + RQA)	0.887	0.840	0.960	0.90
(BPM + Pitch Frequency + Chroma + RQA) top-10 features	0.910	0.860	0.980	0.914
(BPM + Pitch Frequency + Chroma + RQA) **top-5** features	**0.943**	**0.980**	**0.910**	**0.940**

Table 3 Shows of the top-1 accuracy of different feature combinations

VII. RESULTS

The fine-tuned Gradient boosting classifier was tested on the test data set. The proposed hybrid method performs with diagnostic accuracies of 94.3% on the test data set. Fig. 11 shows the confusion matrices for of the Gradient boosting classifier. The F1-score, Precision, and Recall of the tuned Gradient boosting classifier is shown in Table 4

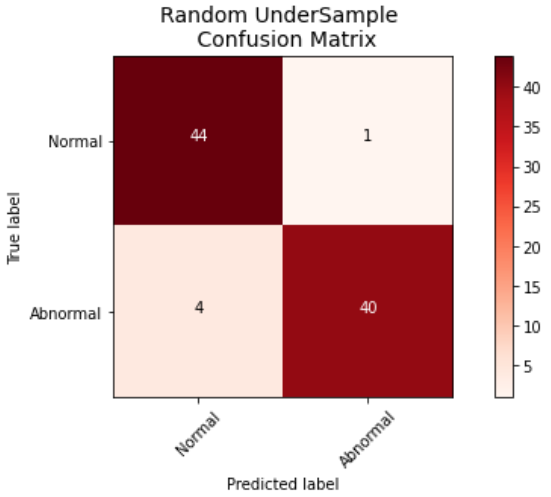

Fig 11. Confusion plot of test sample

	Precision	Recall	F1-score
Normal	0.92	0.98	0.95
Abnormal	0.98	0.91	0.94

Table 4 shows the precision and recall of final model

VIII. Conclusion and Future Work

In this paper, we proposed a machine learning based FHR classification approach using a Gradient boosting classifier. Further, the research focuses on collecting more data, improving the model performance, and implementing different pre-processing techniques to make the classifier more generalized and accurate. Since deep learning networks need many training samples, with sufficient data, recurrent neural network (RNN) architectures such as bidirectional RNN, gated recurrent units (GRU's), and long short-term memory (Lstm) can be implemented in the future. The adaptation of this research can aid the development of a low-cost, safe, and commercially available solution for long-term fetal health monitoring. The end goal of this research is to create a low-cost electronic device that can measure fetal heart signals and accurately predict the fetal health.

IX. Reference

[1] AMIR SWEHA , Interpretation of the Electronic Fetal Heart Rate During Labor 1999 May.

[2] J. A. Martin, B. E. Hamilton, P. D. Sutton, S. J. Ventura, F. Menacker, and M. L. Munson, "Birth: Final data for 2002," Nat.Vital Statist. Report, vol. 52, pp. 1–102, 2003.

[3] Takeuchi, Y.; Hogaki, N. Autocorrelation method for fetal heart ratemeasurement from ultrasonic Doppler fetal signal. In Ultrasound in Medicine; White, D., Brown, R.E., Eds.; Plenum Press: New York, 1977; Vol. 3B "Engineering Aspect", pp. 1327-1332.

[4] R. K. Freeman, T. J. Garite, M. P. Nageotte, and L. A. Miller, Fetal Heart Rate Monitoring. Philadelphia, PA, USA: Lippincott Williams and Wilkins, 2012.

[5] G. A. Macones, G. D. V. Hankins, C. Y. Spong, J. Hauth, and T. Moore, "The 2008 National Institute of Child Health and Human Development workshop report on electronic fetal monitoring: Update on definitions, interpretation, and research guidelines," J. Obstetric, Gynecologic, Neonatal Nursing, vol. 37, no. 5, pp. 510–515, 2008.

[6] NIH. Electronic fetal heart rate monitoring: research guidelines for interpretation. National Institute of Child Health and Human Development Research Planning Workshop. Am J Obstet Gynecol Dec1997;177(6):1385–1390

[7] FIGO Guidelines for the use of fetal monitoring.International Journal of Gynecology Obstetrics 1986;25:159–167.

[8] Kahankova, R., Kolarik, J., Martinek, R., & Durikova, A. (2019). A Comparative Analysis of Fetal Phonocardiograph Acoustical Performance. In IFAC-PapersOnLine (Vol. 52, Issue 27, pp. 514–519). Elsevier BV. https://doi.org/10.1016/j.ifacol.2019.12.715

[9] Hong Tang, Ting Li, Tianshuang Qiu and Yongwan Par, Fetal Heart Rate Monitoring from Phonocardiograph Signal Using Repetition Frequency of Heart Sounds, Volume 2016 |Article ID 2404267

[10] Hong Tang, Ting Li, Tianshuang Qiu and Yongwan Par, Fetal Heart Rate Monitoring from Phonocardiograph Signal Using Repetition Frequency of Heart Sounds, Volume 2016 |Article ID 2404267

[11] V. Chudá cek, "Automatic analysis of intrapartum fetal heart rate," Ph.D. dissertation, Dept. Cybern., Czech Tech. Univ., Prague, Czech Republic, 2011. J. Pardey, M. Moulden, and C. W. Redman, "A computer system for the numerical analysis of nonstress tests," Amer. J. Obstetrics Gynecol., vol. 186, no. 5, pp. 1095–1103,2002

[12] J. Spilka, V. Chudá cek, M. Kouck ˇ y, L. Lhotsk ´ a, M. Huptych, P. P. Janku, ´ G. Georgoulas, and C. Stylios, "Using nonlinear features for fetal heart rate classification," Biomed. Signal Process. Control, vol. 7, no. 4, pp. 350–357, 2011.

[13] A. Reddy, M. Moulden, and C. W. G. Redman, "Antepartum frequency fetal heart rate sinusoidal rhythm: Computerized detection and fetal anemia," Amer. J. Obstetrics Gynecol., vol. 200, no. 4, pp. 407.e1–407.e6, 2009.

[14] P. A. Warrick, E. F. Hamilton, D. Precup, and R. E. Kearney, q"Classification of normal and hypoxic fetuses from systems modeling of intrapartum cardiotocography," IEEE Trans. Biomed. Eng., vol. 57, no. 4, pp 771–779, Apr. 2010

[15] V. S. Chourasia and A. K. Mittra, "Wavelet-based denoising of fetal phonocardiographic signals," Int. J. Med. Eng. Inform., vol. 2, no. 2, pp. 139–150, 2010.

[16] E. Koutsiana, L. J. Hadjileontiadis, I. Chouvarda, and A. H. Khandoker, "Detecting fetal heart sounds by means of Fractal Dimension analysis in the Wavelet domain," Proc. Annu. Int. Conf. IEEE Eng. Med. Biol. Soc. EMBS, pp. 2201–2204, 2017.

[17] F. Kovâcs, M. Török, and I. Habermajer, "A rule-based phonocardiographic method for long-term fetal heart rate monitoring," IEEE Trans. Biomed. Eng., vol. 47, no. 1, pp. 124–130,2000.

[18] S. Dash, J. G. Quirk, and P. M. Djuric, "Fetal heart rate classification using generative models," IEEE Trans. Biomed. Eng., vol. 61, no. 11, pp. 2796–2805, 2014.

[19] Y. Noguchi, F. Matsumoto, K. Maeda, and T. Nagasawa "Neural network analysis and evaluation of the fetal heart rate," Algorithms, vol. 2, no. 1, pp. 19–30, 2009.

[20] V. Chudá cek, J. Spilka, B. Rubackova, M. Koucky, G. Georgoulas, L.Lhotska, and C. Stylios, "Evaluation of feature subsets for classification of cardiotocographic recordings," in Proc. Comput. Cardiol., 2008, pp.845–848.

[21] Emad Haque, Tanishka Gupta, Vinayak Singh, Kaustubh Nene and Akhil Masurkar, Detection and Classification of Fetal Heart Rate (FHR)

[22] M. Samieinasab and R. Sameni, "Fetal phonocardiogram extraction using single channel blind source separation," ICEE 2015 - Proc. 23rd Iran. Conf. Electr. Eng., vol. 10, pp. 78– 83, 2015.

[23] H. Liang, S. Lukkarinen, and I. Hartimo, "Heart sound segmentation algorithm based on heart sound envelogram," Comput. Cardiol., no. September, pp. 105–108, 1997.

[24] H. Beyramienanlou and N. Lotfivand, "Shannon's Energy Based Algorithm in ECG Signal Processing," Comput. Math. Methods Med., vol. 2017, 2017.

[25] X. Liu and L. Bo, "Identification of resonance states of rotor- bearing system using RQA and optimal binary tree SVM,"Neurocomputing, vol. 152, no. 1, pp. 36–44, 2015.

[26] F. Takens, "Detecting strange attractors in turbulence," Lec- ture Notes in Mathematics, vol. 898, no. 1, pp. 366–381, Springer, Berlin, Heidelberg, 1981.

[27] Z. Ma, G. Wen, and C. Jiang, "EEMD independent extraction for mixing features of rotating machinery reconstructed in phase space," Sensors, vol.15, no. 4, pp. 8550–8569, 2015.